Electronic Supplementary Material (ESI) for Materials Chemistry Frontiers.

Supporting Information

Coupling the BODIPY with Nitrogen-Doped Graphene Quantum Dot to Address Water Solubility of Photosensitizers

I. Jénnifer Gómez,*[,a] Marina Russo,[b,c] Orazio Angelo Arcidiacono,[d,e] Esther M. Sánchez-Carnerero,[b,c] Petr Klán[b,c] and Lenka Zajíčková*[,a,f]

[a.] *Department of Condensed Matter Physics, Faculty of Science, Masaryk University, Kotlářská 2, 611 37 Brno, Czech Republic*

[b.] *Department of Chemistry, Faculty of Science, Masaryk University, Kamenice 5, 62500 Brno, Czech Republic.*

[c.] *RECETOX, Faculty of Science, Masaryk University, Kamenice 5, 62500 Brno, Czech Republic.*

[d.] *Institute of Biophysics of the Czech Academy of Sciences, Královopolská 135, 61265 Brno, Czech Republic.Department of Chemistry, Faculty of Science, Masaryk University, Kamenice 5, 625 00 Brno, Czech Republic*

[e.] *Department of Experimental Biology, Faculty of Science, Masaryk University, Kamenice 5, 62500 Brno, Czech Republic.*

[f.] *Central European Institute of Technology – CEITEC, Brno University of Technology, Purkyňova 123, 61200 Brno, Czech Republic.*

Table of Contents

1. Materials and Methods

1.1. Reagents and Materials

The reagents and solvents of the highest purity were used as supplied, or they were purified/dried using the standard methods when necessary. Dialysis membrane tubes with a 0.5-1 kDa cut-off were supplied by Spectrum Labs (USA). Ultrapure water used in all experiments was produced using a Milli-Q water system (Millipore, Merck, Germany). Annexin V, 7-aminoactinomycin D (7-AAD) staining, and a CellROX Deep Red reagent were purchased from Thermo Fisher (USA). HeLa cells were supplied from American Type Culture Collection (USA).

1.2. Chemical Analyses

The free amino groups of GQDs were determined by the Kaiser test using a commercial kit.[1] The Kaiser test is based on an intense blue color generated by the reaction of ninhydrin with free primary amines, which is then evaluated spectrophotometrically. NGQDs-BODIPY-I (1.2 mg) or NGQDs-BODIPY-Br (1.1 mg) was added to a solution containing 75 µL of a solution 1 (80 g of phenol in 20 mL of ethanol), 100 µL of a solution of 2 (2 mL of KCN 1 mM in water in 98 mL of pyridine), and 75 µL of a solution 3 (1 g of ninhydrin in 20 mL of ethanol). The mixture was heated at 120 ^{o}C for 10 min and finally diluted with ethanol (60%) to obtain the final volume of 3 mL. For the quantitative determination of free amino groups on the surface of dots, the absorbance was recorded at 570 nm, setting the zero on the blank without sample. The ratio between the moles of the primary amine moiety and the weight of the sample is given by:

$$[NH_2] = \frac{A_{570} \cdot V}{\varepsilon \cdot m} \quad \ldots(1)$$

where A_{570} is the absorbance at 570 nm, V is the final volume after dilution (3 mL), ε is the molar absorption coefficient (15000 M^{-1} cm^{-1}), and m is the mass of NGQD-BODIPYs.

2. Synthetic Procedures

NGQDs

NGQDs were synthesized according to our previously reported method.[2] A bottom-up technique in a Discover SP microwave (CEM, USA) with the assisted hydrothermal method was used. Glucose (25 mg, 0.14 mmol.) was dissolved in 1 mL of milli-Q water, followed by the addition of ethylenediamine (21.40 µL, 0.32 mmol). The solution was heated in a microwave reactor at 200 W for 150 s to grow N-GQDs. The N-GQDs samples were filtrated by a microporous filter of 0.1 µm to remove the excess of unreacted compounds. Afterwards, the N-GQDs were dialyzed by molecular weight cut-off of 0.5-1 KDa against pure water for 2 days.

BODIPY Derivatives

8-Carboxy-4,4'-difluoro-2,6-diiodo-1,3,5,7-tetramethyl-4-bora-3a,4a-diaza-s-indacene (BODIPY-I) was prepared according to a procedure described in the literature.[3] 4,4'-Difluoro-2,6-diiodo-8-methoxycarbonyl-1,3,5,7-tetramethyl-4-bora-3a,4a-diaza-*s*-indacene[3] (0.100 g, 0.179 mmol, 1 equiv) was dissolved in dry ethyl acetate (50 mL) and LiI (0.240 g, 1.79 mmol, 10 equiv.) was added. The reaction mixture was refluxed under a nitrogen atmosphere for 15 h. TLC was used to monitor the reaction. When the reaction was finished, the mixture was cooled to room temperature, and a small amount of HCl (0.2 mL) was added to quench the reaction. Water was added, and the mixture was extracted with ethyl acetate (3 × 10 mL).

The combined organic layers were washed with water (20 mL), dried over anhydrous sodium sulfate, filtered, and concentrated to dryness under reduced pressure. The compound was purified by flash chromatography (ethyl acetate/methanol, 9:1). Yield 0.071 g (73%). Red solid. ^{1}H NMR (300 MHz, CD_3OD): δ (ppm) 2.53 (s, 6 H), 2.38 (s, 6H). ^{13}C NMR (125 MHz, CD_3OD): δ (ppm) 170.5, 156.4, 145.0, 141.0, 129.0, 84.0, 16.0, 15.6. The spectroscopic data are in good agreement with those reported in the literature.[3]

2,6-Dibromo-8-Carboxyl-4,4'-difluoro-1,3,5,7-tetramethyl-4-bora-3a,4a-diaza-s-indacene (BODIPY-Br) was prepared according to a procedure described in the literature.[3] 8-Carboxy-4,4'-difluoro-1,3,5,7-tetramethyl-4-bora-3a,4a-diaza-*s*-indacene[3] (0.04g, 0.14 mmol, 1 equiv.) was solved in a mixed solution of dichloromethane/DMF (1:1), and NBS (0.05 g, 0.29 mmol, 2.1 equiv.) was added. The solution was stirred at room temperature for 4 h. The reaction was quenched with water, and the organic matter was extracted with dichloromethane. The organic layers were washed with water, dried over anhydrous magnesium sultafe, filtered, and the solvent was evaporated under reduced pressure. The crude mixture was purified by flash chromatography (ethyl acetate/methanol, 9:1 to 7:1). Yield 0.03 g (49%). Orange powder. ^{1}H NMR (300 MHz, CD_3OD): δ (ppm) 2.50 (s, 6H), 2.36 (s, 6H). ^{13}C NMR (125 MHz, CD_3OD): δ (ppm) 170.2, 153.4, 141.5, 140.3, 128.1, 110.8, 13.6, 12.4. The spectroscopic data are in good agreement with those reported in the literature.[3]

NGQD-BODIPY Photosensitizers

NGQD-BODIPY-I. 1-Ethyl-3-(3-dimethylaminopropyl)carbodiimide (EDC, 3.52 mg, 0.018 mmol, 2 equiv.) and *N*-hydroxysuccinimide (NHS ,2.12 mg, 0.018 mmol, 2 equiv.) were added to a solution of BODIPY-I (5 mg, 0.009 mmol, 1 equiv.) in DMF (5 mL). The mixture was stirred at 0 °C for 1 h. Afterwards, NGQDs (18.65 mg) were added, and the resulting mixture was stirred at room temperature for 16 h. The solvent was removed under reduced pressure, and the crude mixture was dissolved in methanol and isolated by size exclusion chromatography using a column packed with Sephadex LH20 (eluting with methanol). Finally, the solvent was removed under reduced pressure to obtain NGQD-BODIPY-I (14.9 mg) as an orange powder. The qualitative analysis data are shown below.

NGQD-BODIPY-Br. EDC (5.13 mg, 0.027 mmol, 2 equiv.) and NHS (3.08 mg, 0.027 mmol, 2 equiv.) were added to a solution of BODIPY-Br (6 mg, 0.014 mmol, 1 equiv.) in DMF (5 mL). The mixture was stirred at 0 °C for 1 h. Afterwards, NGQDs (27 mg) were added, and the resulting mixture was stirred at room temperature for 16 h. The solvent was removed under reduced pressure, and the crude mixture was dissolved in methanol and isolated by size exclusion chromatography using a column packed with Sephadex LH20 (eluting with methanol). Finally, the solvent was removed under reduced pressure to obtain NGQD-BODIPY-Br (20.3 mg) as a brownish powder. The qualitative analysis data are shown below.

3. Supporting Photographs

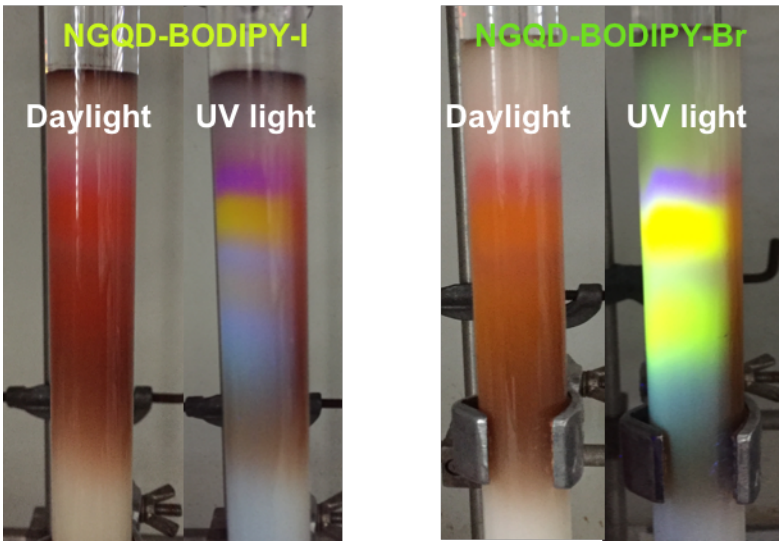

Figure S1. Separation and purification of NGQD-BODIPY PSs using size exclusion chromatography (SEC). The separated bands are visualized under ambient light and 365 nm excitation UV lamp, respectively.

4. XPS Measurements

The chemical composition of NGQD-BODIPY-I were analyzed by the fitting of high-resolution B 1s, C 1s, N 1s, O 1s, I 3d, and F 1s XPS signals. The grafting of the BODIPY-I onto the surface of dots was confirmed through the detection of a high resolution B 1s at 192 eV, I $3d_{5/2}$ at 620 eV, I $3d_{3/2}$ at 632 eV and F 1s at 686 eV (Figure S2, Figure S5 and Figure S6, Table S1, respectively).[4–6] Furthermore, C 1s was composed of four components corresponding to the C–C/C=C (284eV), C–O/C–N/C–I (286 eV), C=O/C=N (2867 eV), and COOH bonds (288 eV) (Figure S3 and Table S1). Deconvolution of the high resolution O 1s peak revealed three components corresponding to the O=C (531 eV), O–C (532 eV) and C–O–C (533 eV) bonds (Figure S4 and Table S1).

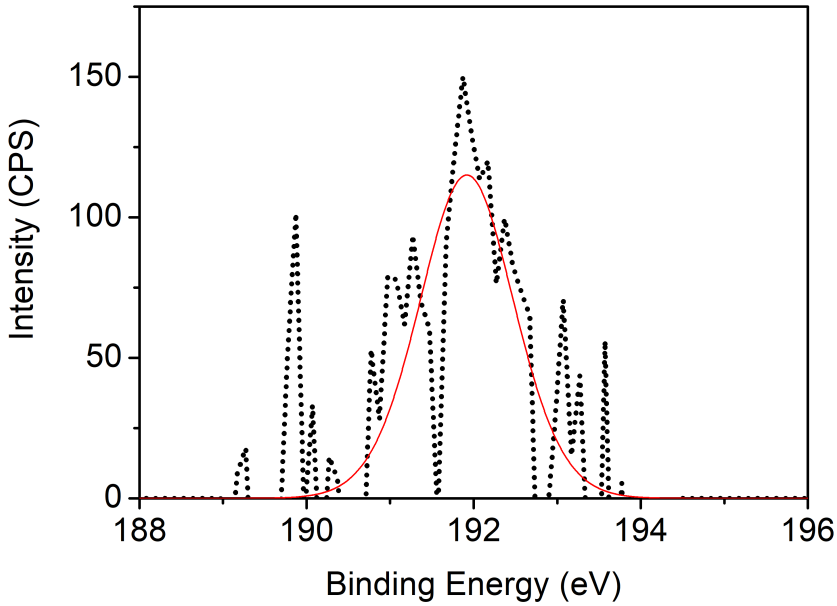

Figure S2. High-resolution XPS spectra of B 1s in NGQD-BODIPY-I.

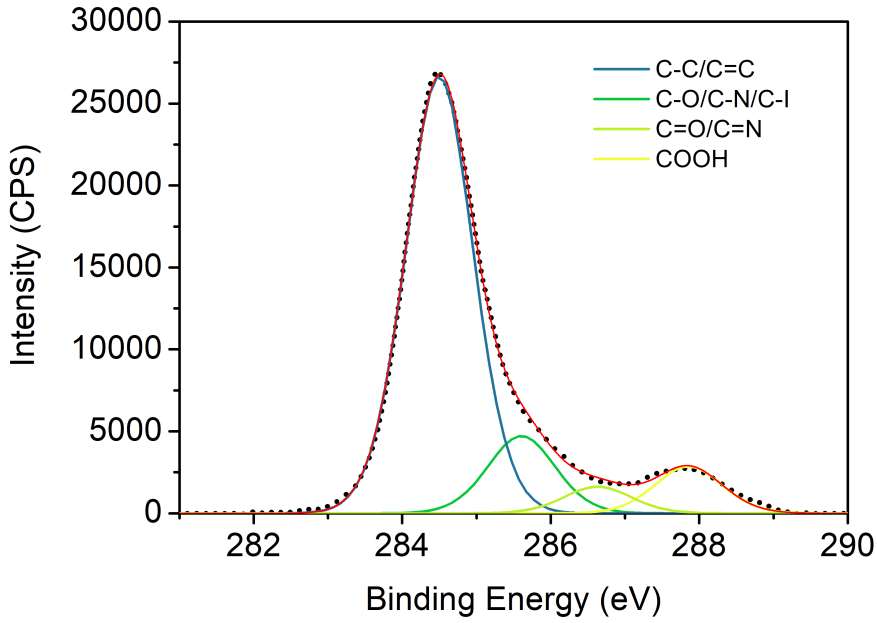

Figure S3. High-resolution XPS spectra and the deconvolution of C 1s in NGQD-BODIPY-I.

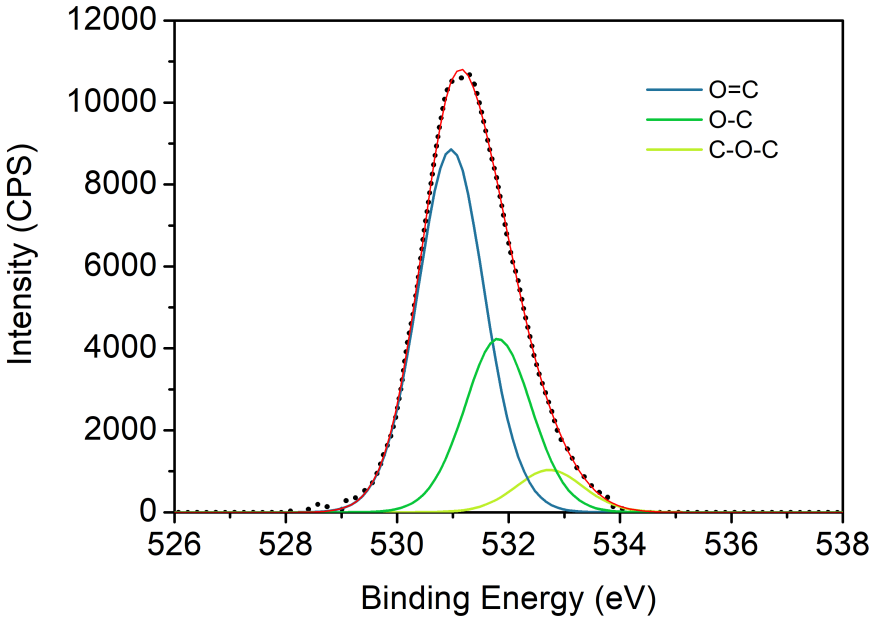

Figure S4. High-resolution XPS spectra and the deconvolution of O 1s in NGQD-BODIPY-I.

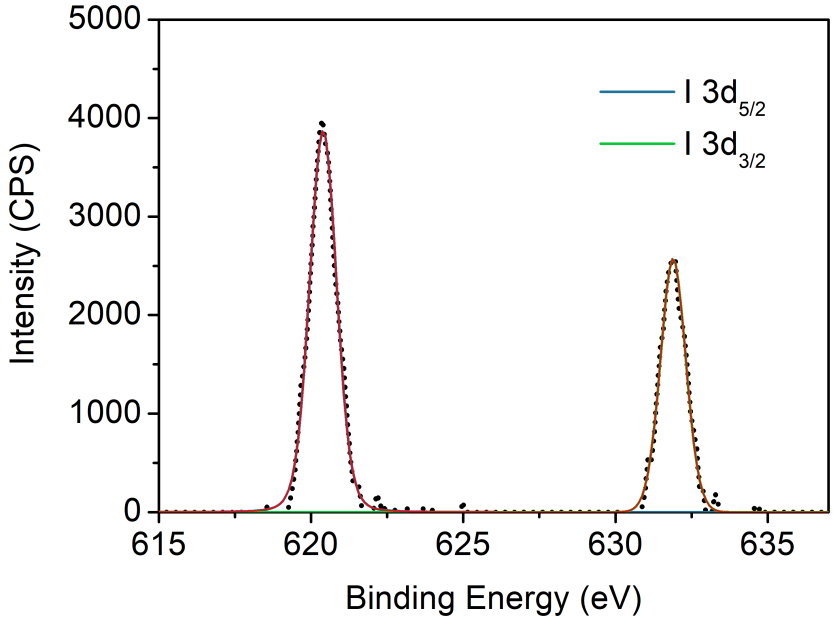

Figure S5. High-resolution XPS spectra of I 3d in NGQD-BODIPY-I.

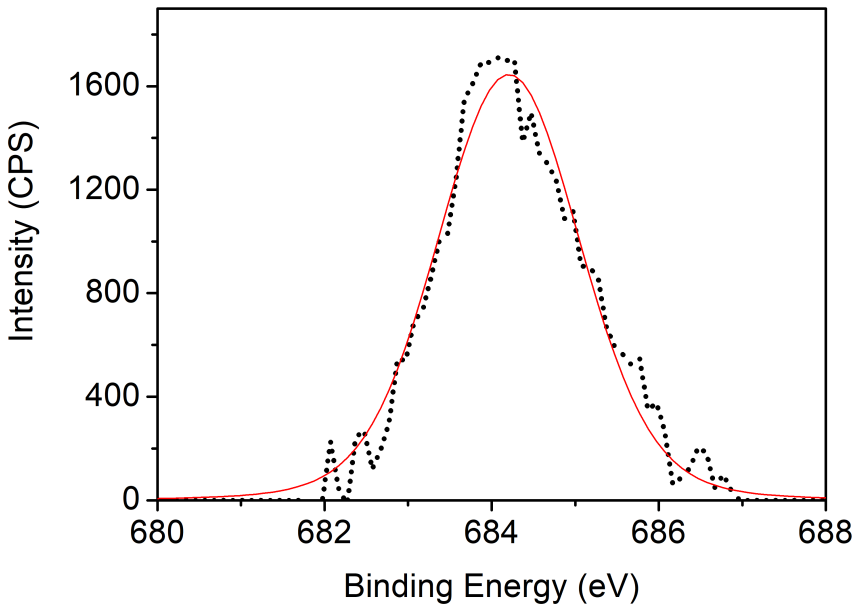

Figure S6. High-resolution XPS spectra of F 1s in NGQD-BODIPY-I.

Table S1. Atomic composition and binding energies of B, C, N, O, I and F in NGQD-BODIPY-I as determined by XPS.

Core level	Binding Energy (eV)	Atomic (%)
B 1s	**191.87**	**0.49**
C 1s	**284.47**	**78.91**
C-C/C=C	284.50	74.32
C-O/C-N/C-I	285.60	13.15
C=O/C=N	286.63	4.54
COOH	287.86	7.99
N 1s	**399.17**	**4.74**
N=C	399.33	82.08
N-H_2/C-N-C	400.92	11.07
N-C_3	401.71	6.85
O 1s	**531.27**	**13.72**
O=C	530.97	62.70
O-C	531.81	29.97
C-O-C	532.73	7.33
I 3d	**620.37**	**0.67**
I $3d_{5/2}$	620.40	59.51
I $3d_{3/2}$	631.89	40.49
F 1s	**684.07**	**1.47**

Following the above premises, the chemical bonds for NGQD-BODIPY-Br were analyzed by the fitting of the high-resolution Br 3d, B 1s, C 1s, N 1s, O 1s, and F 1s XPS signals. The grafting of the BODIPY-Br onto the surface of the dots was confirmed through the detection of high resolution Br 3d at 70 eV, B 1s at 190 eV and F 1s at 686 eV, as it is commented in the main manuscript (see also Figure S7, Figure S8 and Figure S11, Table S2).[4–7] In detail, the deconvolution of the high resolution C 1s peak resulted in four components corresponding to the C–C/C=C (284eV), C–O/C–N/C–Br (286 eV), C=O/C=N (2867 eV), and COOH moietis (288 eV) (Figure S9 and Table S2). The O 1s peak revealed three components corresponding to the O=C (531 eV), O–C (532 eV) and C–O–C (533 eV) bonds (Figure S10 and Table S2).

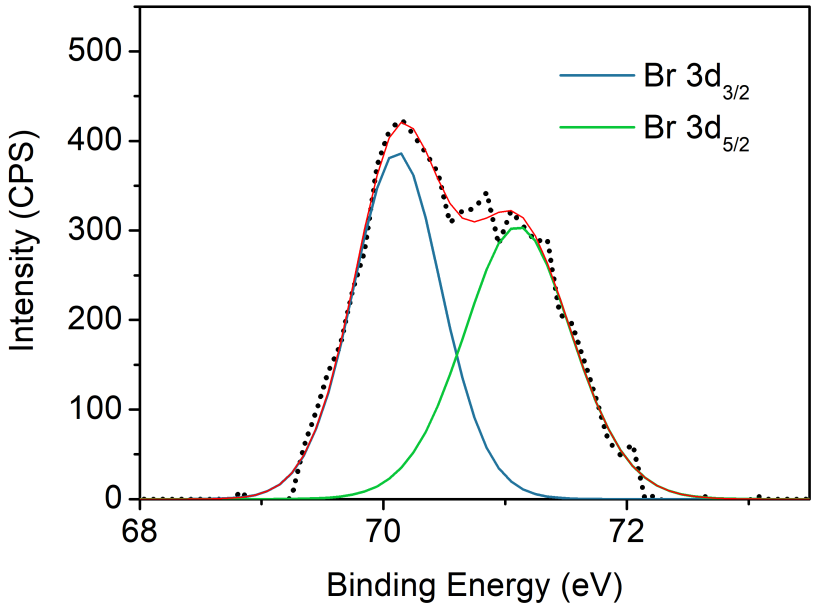

Figure S7. High-resolution XPS spectra of Br 3d NGQD-BODIPY-Br.

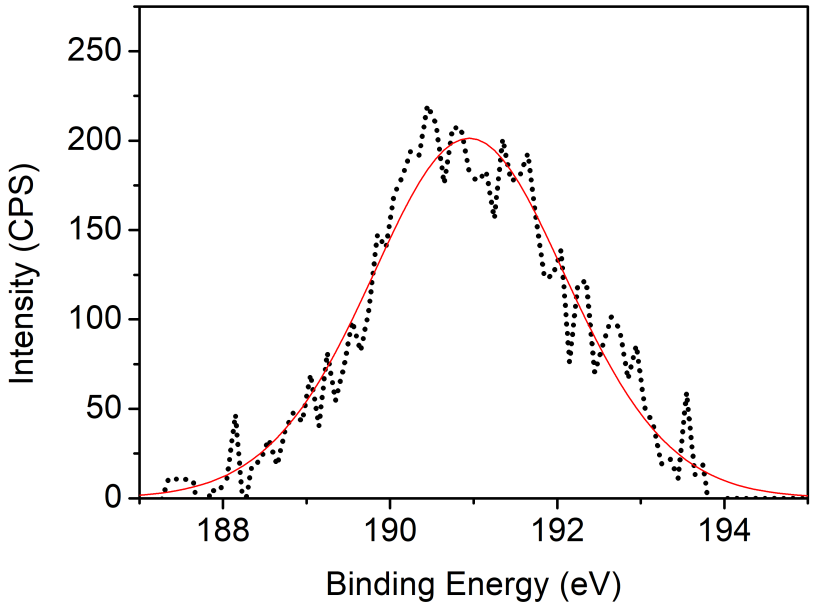

Figure S8. High-resolution XPS spectra of B 1s NGQD-BODIPY-Br.

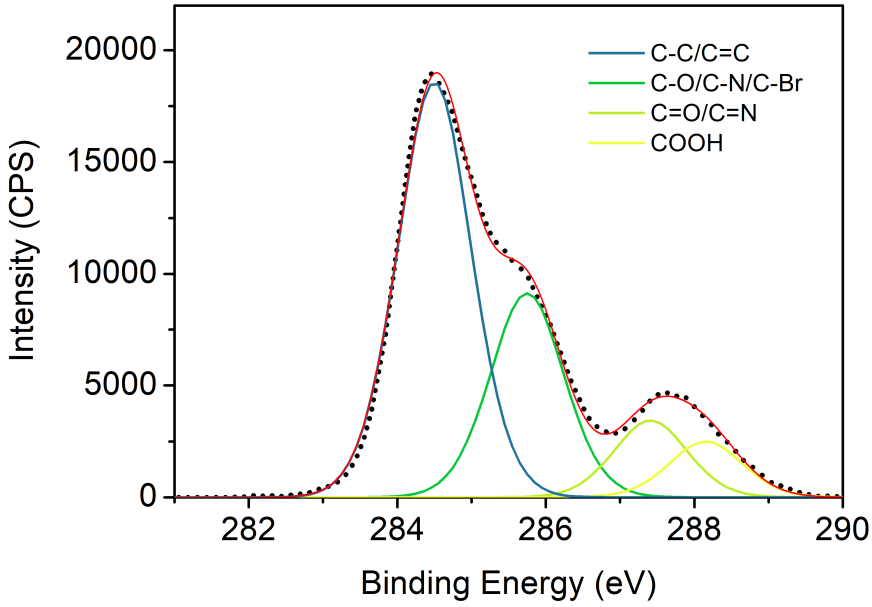

Figure S9. High-resolution XPS spectra and the deconvolution of C 1s in NGQD-BODIPY-Br.

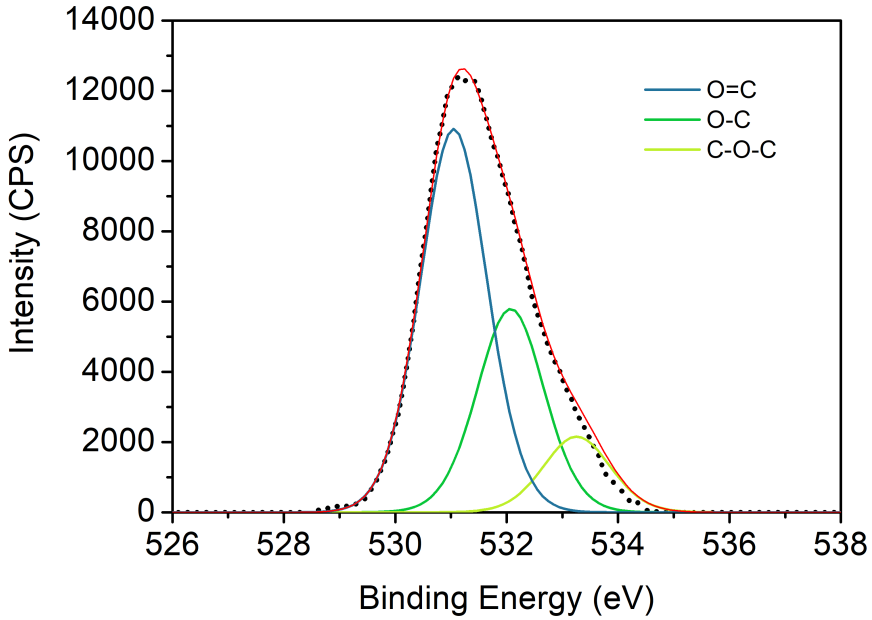

Figure S10. High-resolution XPS spectra and the deconvolution of O 1s NGQD-BODIPY-Br.

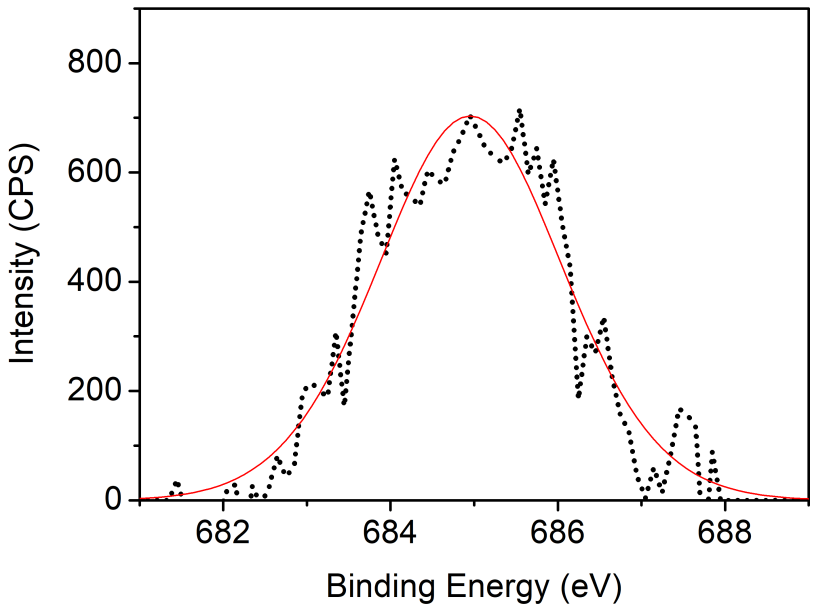

Figure S11. High-resolution XPS spectra of F 1s NGQD-BODIPY-Br.

Table S2. Atomic composition and binding energies of Br, B, C, N, O and F in NGQD-BODIPY-Br as determined by XPS.

Core level	Binding Energy (eV)	Atomic (%)
Br 3d	**70.15**	**0.63**
Br $3d_{3/2}$	70.11	51.10
Br $3d_{5/2}$	71.10	48.90
B 1s	**190.45**	**2.01**
C 1s	**284.45**	**70.09**
C-C/C=C	284.50	55.21
C-O/C-N/C-Br	285.75	27.15
C=O/C=N	287.41	10.21
COOH	288.15	7.43
N 1s	**399.35**	**11.06**
N=C	399.35	77.60
N-H_2/C-N-C	400.88	19.79
N-C_3	402.35	2.61
O 1s	**531.15**	**15.52**
O=C	531.05	57.87
O-C	532.07	30.70
C-O-C	533.26	11.43
F 1s	**685.55**	**0.69**

5. Optical Measurements

Absorption

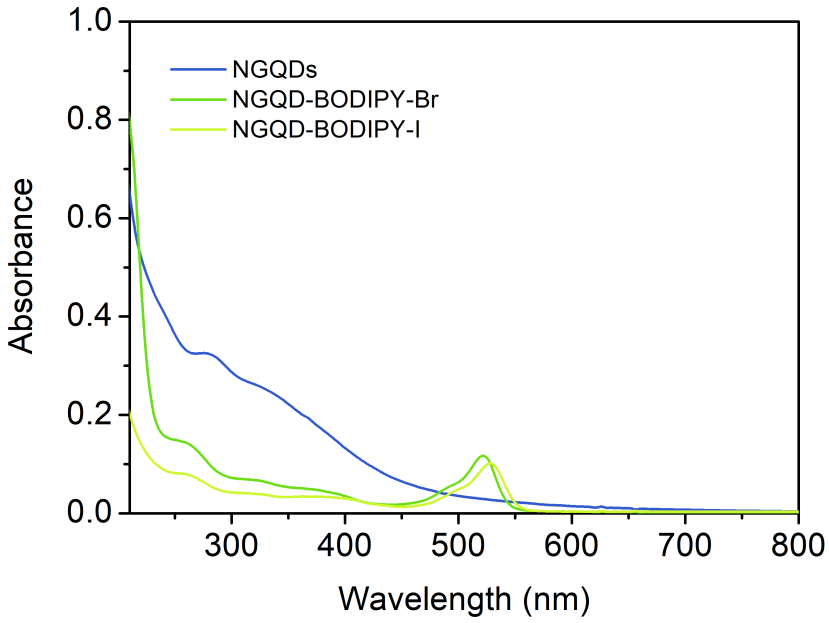

Figure S12. UV-Vis absorption spectra in H_2O.

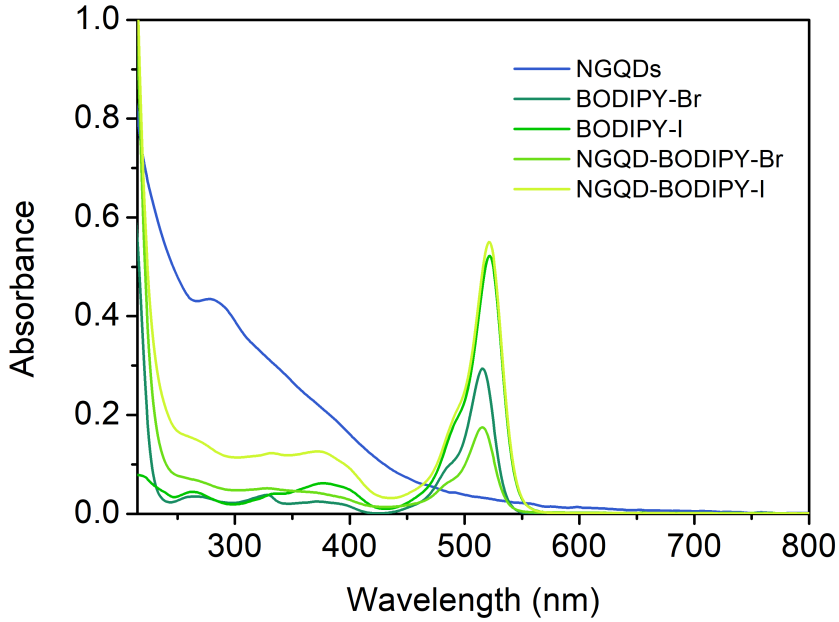

Figure S13. UV-Vis absorption spectra in methanol.

Fluorescence

Table S3. Fluorescence spectroscopic data of the shift in the maximum excitation and emission wavelengths (λ_{ex} and λ_{em}). Data obtained from Figrue 3 and Figure S15.

Sample	λ_{ex} (nm)	λ_{em} (nm)
NGQDs	380	466
NGQD–BODIPY-I	320	420
NGQD–BODIPY-Br	320	417

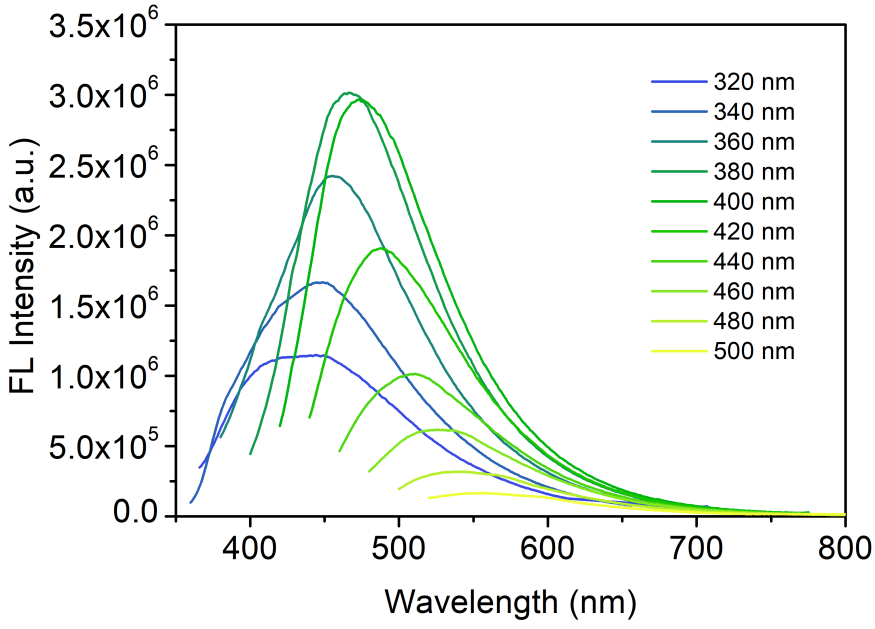

Figure S14. Emission spectra of NGQDs in H_2O at different excitation wavelengths.[2]

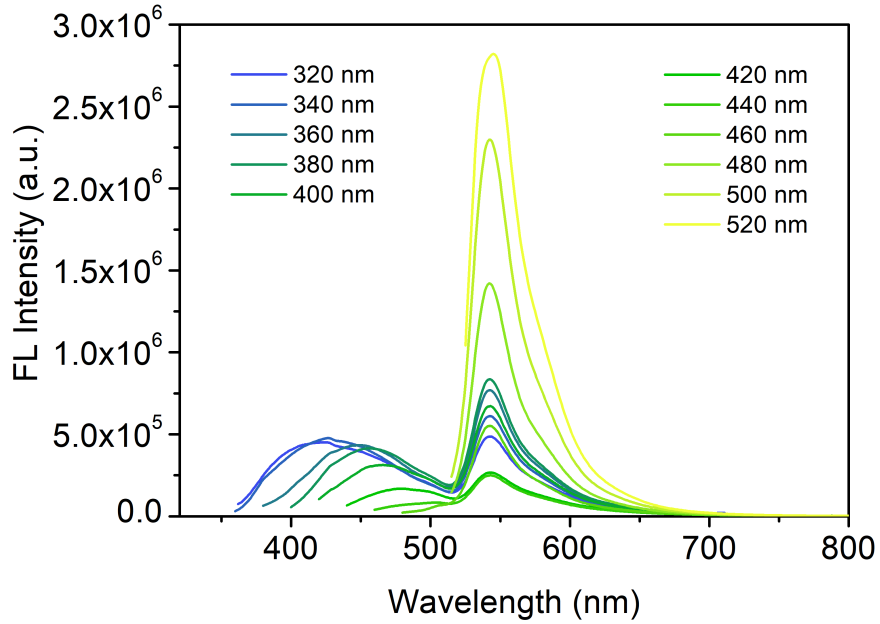

Figure S15. Emission spectra of NGQD-BODIPY-I in methanol at different excitation wavelengths.

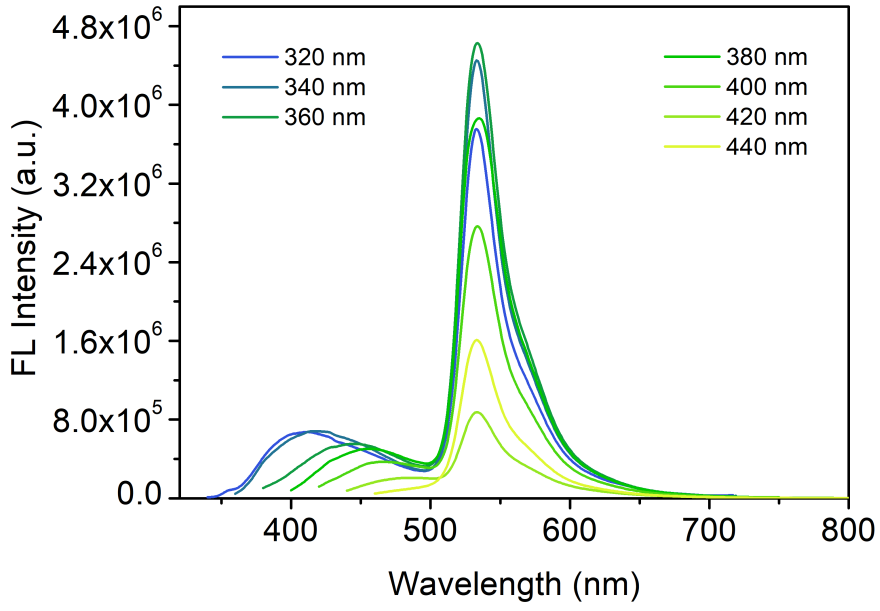

Figure S16. Emission spectra of NGQD-BODIPY-Br in methanol at different excitation wavelengths.

6. Singlet Oxygen Measurements

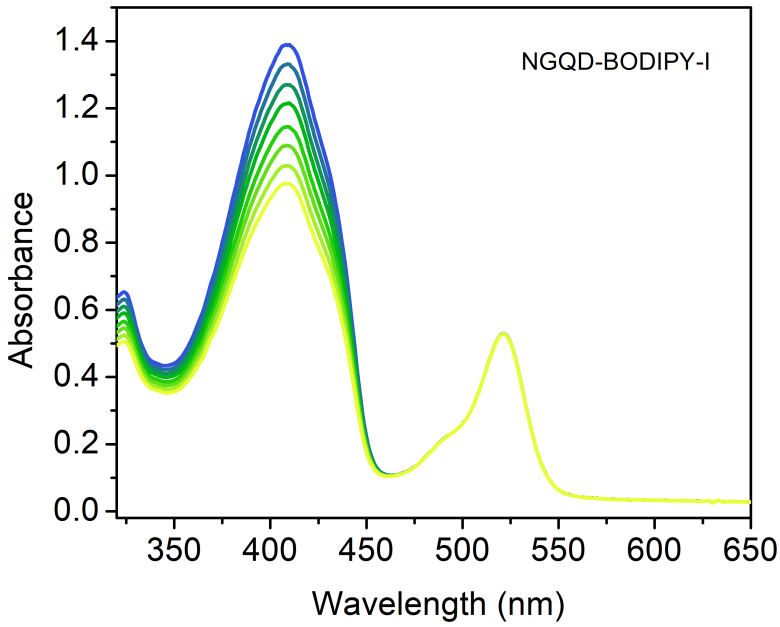

Figure S17. Absorption spectra of the reaction of singlet oxygen generated by photosensitization in the presence of 1,3-diphenylisobenzofuran (DPBF) as a $^1O_2$ trap and NGQD-BODIPY-I in methanol (irradiated by LEDs at λ_{max} = 525 nm).

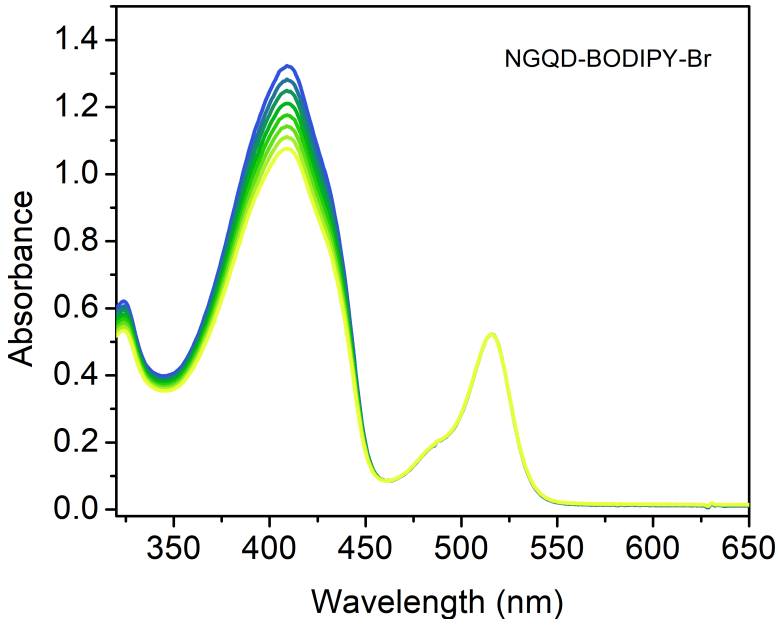

Figure S18. Absorption spectra of the reaction of singlet oxygen generated by photosensitization in the presence of DPBF and NGQD-BODIPY-Br in methanol as a solvent (irradiated by LEDs at λ_{max} = 525 nm).

The hybrid molecule is relatively stable during direct irradiation to the NGQD band after 90 minutes, which suggests that the GQDs motif is not oxidized during irradiation (Figure S19).

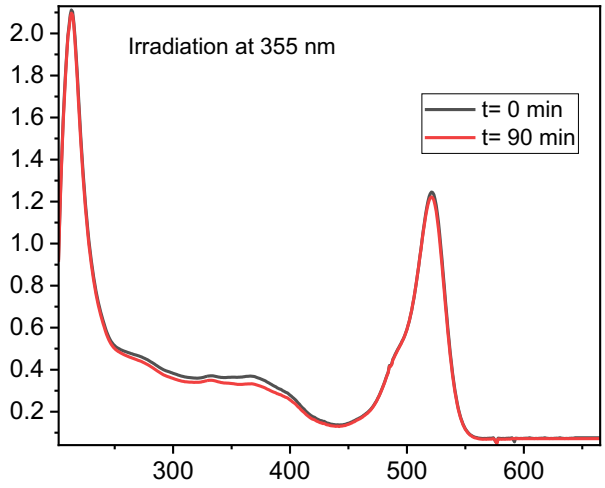

Figure S19. Absorption spectra of NGQD-BODIPY-I under irradiation at 355 nm in H2O.

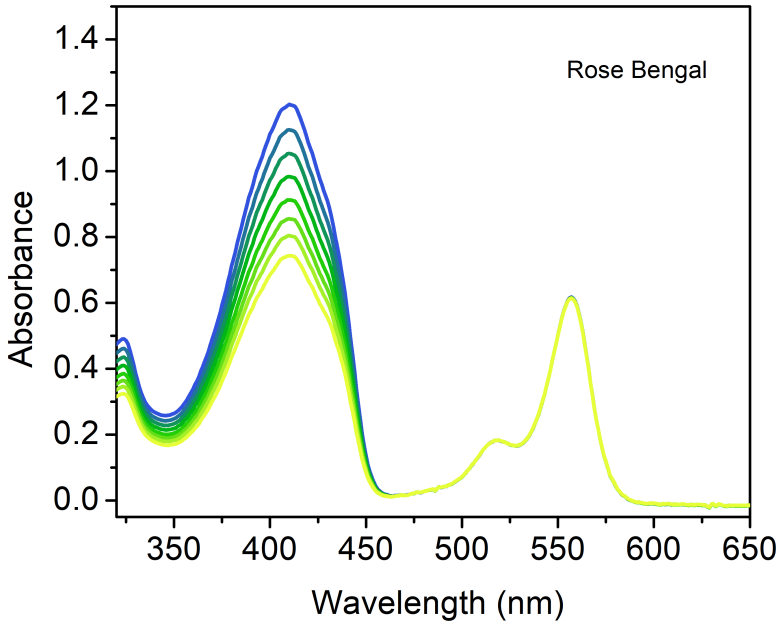

Figure S20. Absorption spectra of the reaction of singlet oxygen generated by photosensitization in the presence of DPBF and rose bengal in methanol as a solvent (irradiated by LEDs at λ_{max} = 525 nm).

The Φ_Δ for NGQD-BODIPY-I and NGQD-BODIPY-Br was found to be 0.68 and 0.49, respectively.

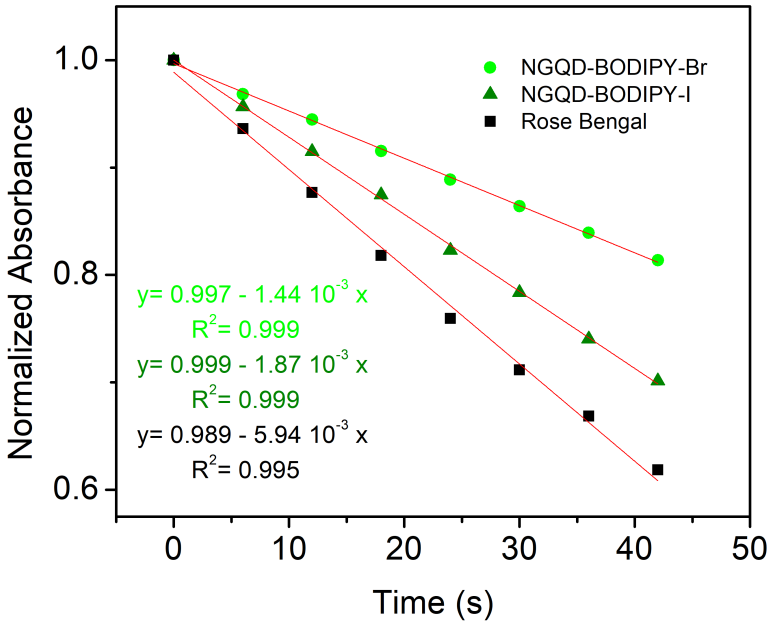

Figure S21. Decomposition rate constant of DPBF in the presence of NGQD-BODIPYs and rose bengal in methanol (irradiated by LEDs at λ_{max} = 525 nm); followed by UV-Vis spectroscopy each 6 s.

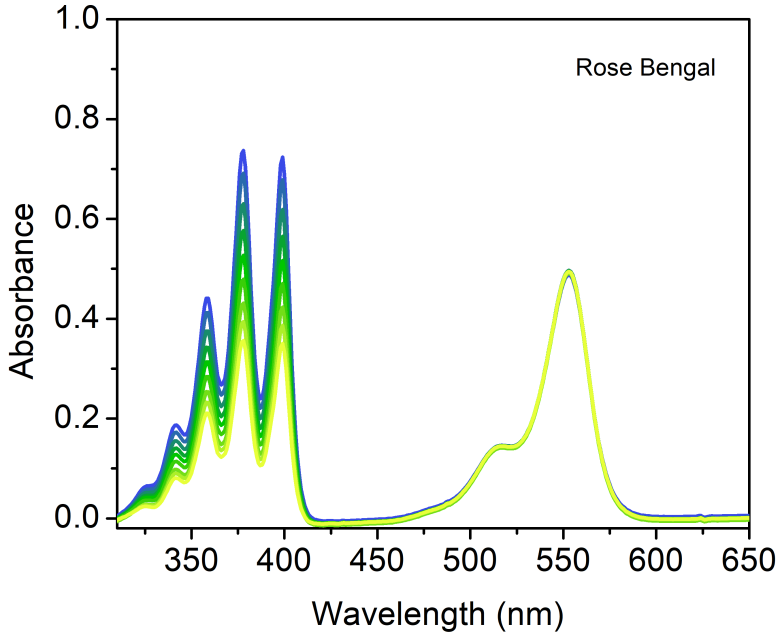

Figure S22. Absorption spectra of the reaction of singlet oxygen generated by photosensitization in the presence of anthracene-9,10-dipropionic acid disodium (ADPA) and rose bengal in H_2O.

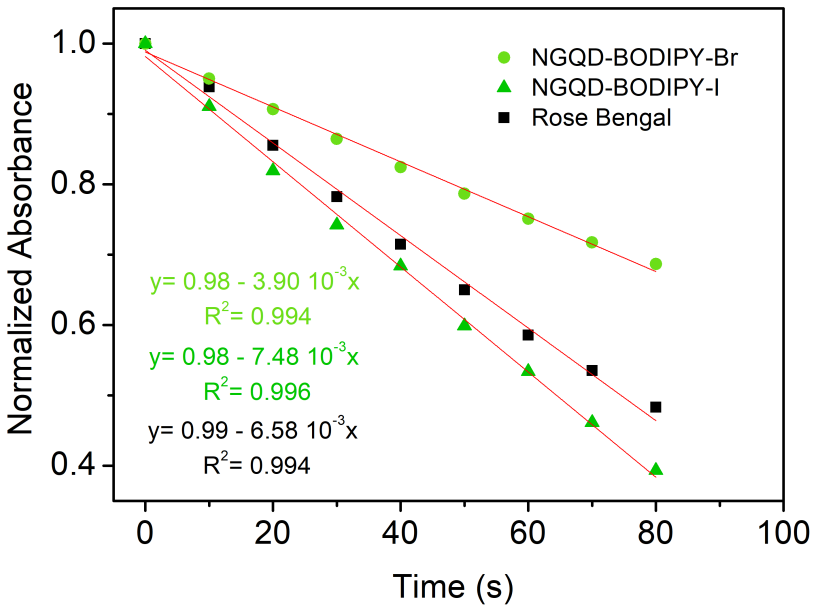

Figure S23. Decomposition rate constant of ADPA in the presence of NGQD-BODIPYs and rose bengal in H_2O (irradiated by LEDs at λ_{max} = 525 nm); followed by UV-Vis spectroscopy each 5 s.

7. *In vitro* Photodynamic Therapy Activity Measurements

Experiment setup

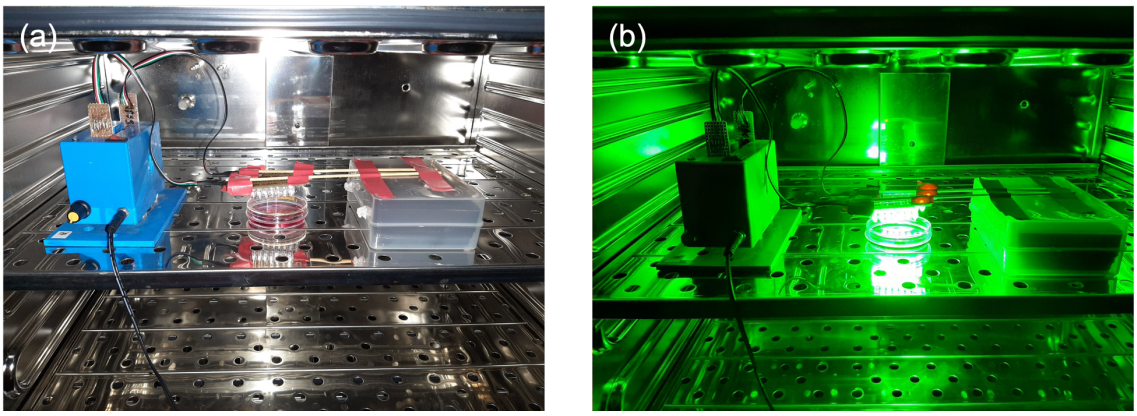

Figure S24. (a) Photographs of the experiment setup and the (b) PDT experiment being performed.

Cell Viability

The following results are expressed as the percentage of alive, necrotic, apoptotic, and late apoptotic cells per treatment compared with untreated control or treated cells without LEDs irradiation (Figure S25). Regarding the irradiation time used on the PDT experiments,[8] an optimization was carried out (data non-shown), and the optimal time of irradiation selected was 10 min using the LEDs (525 nm).

Overall, the apoptosis can take place immediately and/or up to 24 h after the treatment. In these experiments, we used 2 time-points to study the development of cell death. In detail, short and long times after the treatment (6 h and 24 h) were selected.

Irradiation of the samples by LEDs (λ_{max} = 525 nm) for 10 min (Figure S24) led to a high level of cell death (Figure S25). The cell viability gradually decreased as the NGQD-BODIPY concentration increased. Remarkably, a high extent of cell death of ~62% (~7% apoptosis,

~6% necrosis, and ~49% late apoptosis) was found 24 h after the irradiation of solutions with a low (50 μg mL^{-1}) concentration of NGQD-BODIPY-I (Figure S27 and Table S3). However, due to the toxicity presented at high concentrations of NGQD-BODIPY-I, NGQD-BODIPY-Br was selected as a sensitizer for further experiments.

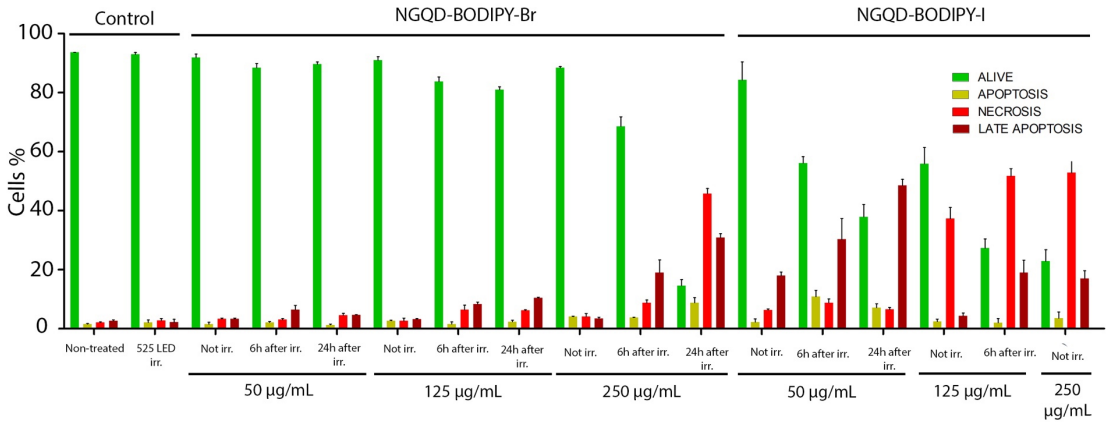

Figure S25. Cell viability of HeLa cells incubated with 50, 125 and 250 μg mL^{-1} of NGQD-BODIPY PSs. Data are the mean of three independent experiments, two-way ANOVA was used for statistical analysis ($p \leq 0.0001$).

Representative Density Plots of the Measurements Carried out by Flow Cytometry

The right lower quadrant in Figures S26–S28 represents annexin V^+/7-AAD negative staining indicating apoptosis. The right upper quadrant represents both high annexin V and 7-AAD staining indicating late apoptosis (staining patterns due to a loss of plasma membrane integrity). The left upper quadrant represents low annexin V and high 7-AAD staining indicating necrosis. The left lower quadrant indicates viable cells. To determine the HeLa viability, the following controls were set to determine the appropriate quadrant allocation in all experiments: untreated cells and untreated LED 525 irradiated cells.

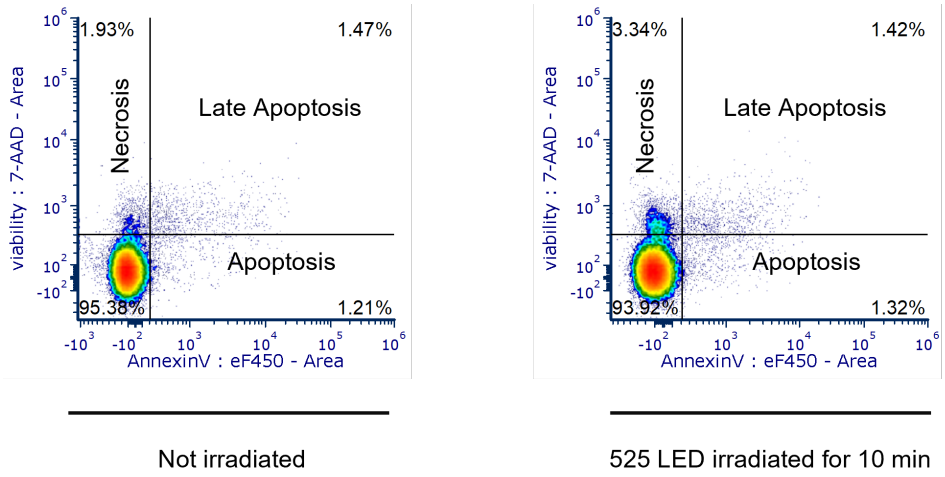

Figusre S26. Flow cytometry density plots showing annexin V (X-axis) and 7-AAD (Y-axis) staining of HeLa cells. Staining per the untreated cells (*i.e.*, control) without LED irradiation and 24 h after LED irradiation (10 min).

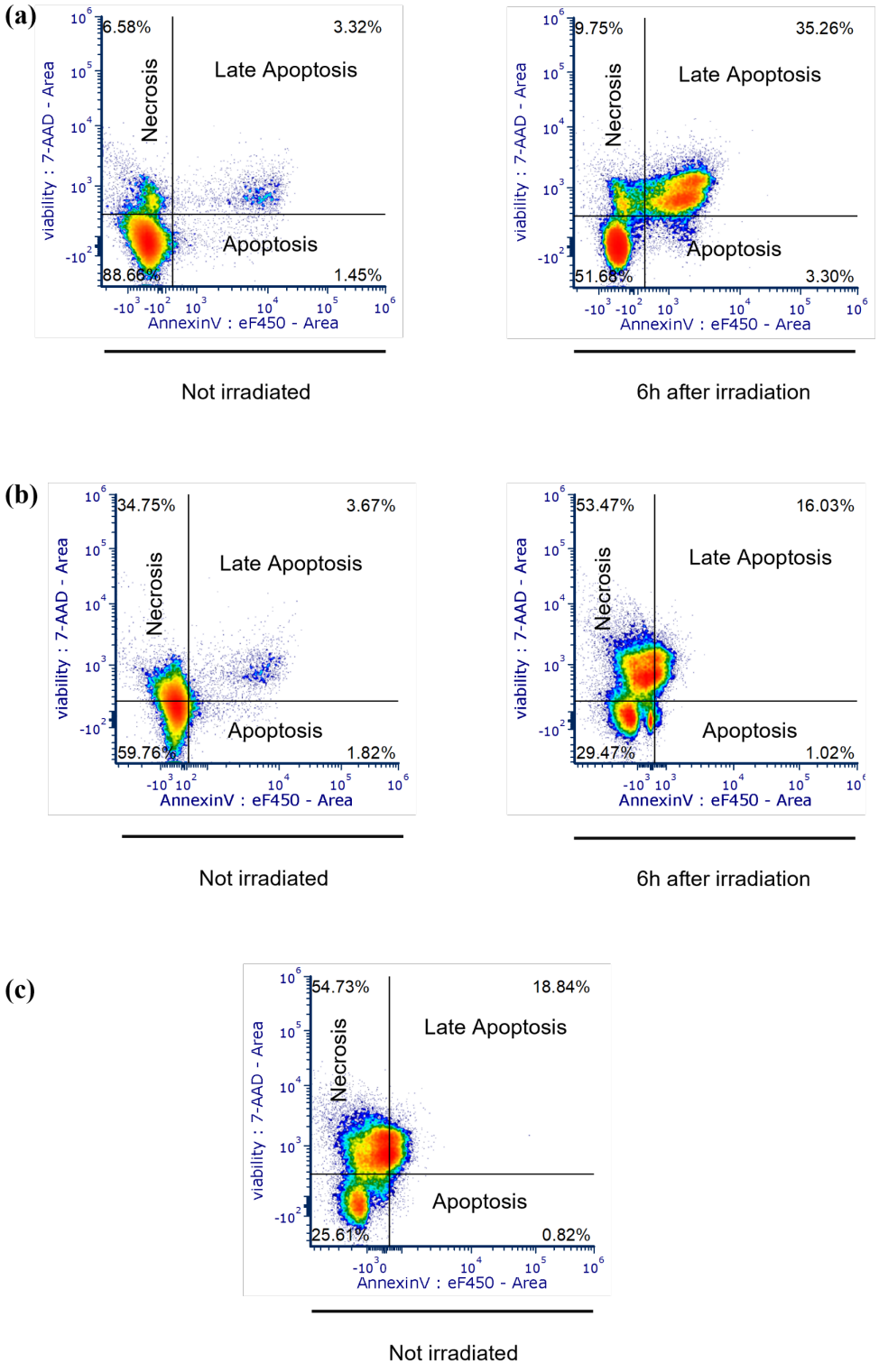

Figure S27. Flow cytometry density plots showing annexin V (X-axis) and 7-AAD (Y-axis) staining of HeLa cells. Staining per each treatment with NGQD-BODIPY-I without LED irradiation and 6 h after LED irradiation. (a) 50 μg mL^{-1}, (b) 125 μg mL^{-1}, and (c) 250 μg mL^{-1}.

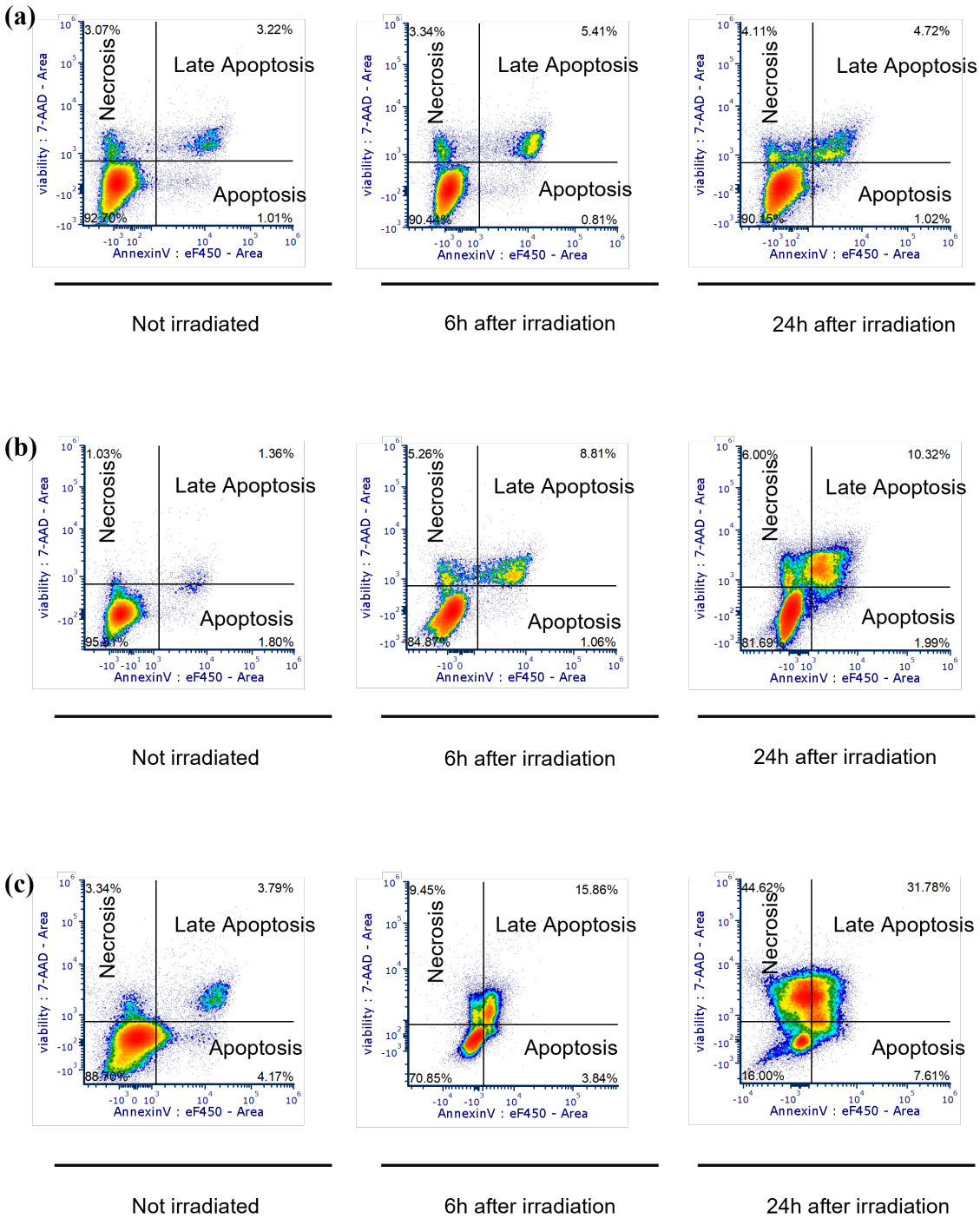

Figure S28. Flow cytometry density plots showing annexin V (X-axis) and 7-AAD (Y-axis) staining of HeLa cells. Staining per each treatment with NGQD-BODIPY-Br without LED irradiation and 6 h and 24 h after LED irradiation. (a) 50 μg mL^{-1}, (b) 125 μg $mL^{-}1$, and (c) 250 μg mL^{-1}.

In summary, the quantitative cell viability results carried out by the flow cytometry (Figures S26–S28) are summarized in Table S3.

Table S4. Percentages of the alive, necrotic, apoptotic, and late apoptotic cells in the synthesized PSs as determined by flow cytometry.

	Alive	Apoptosis	Necrosis	Late apoptosis
CTRL	93.58 ± 0.09	1.59 ± 0.17	2.13 ± 0.18	2.71 ± 0.25
525 LED irr.	92.96 ± 0.62	2.09 ± 0.88	2.75 ± 0.71	2.23 ± 0.96
NGQD-BODIPY-I				
50 μg mL^{-1} not irr.	84.33 ± 4.33	2.23 ± 0.77	6.29 ± 0.29	17.92 ± 0.92
50 μg mL^{-1} irr. after 6 h	56.12 ± 1.56	10.84 ± 1.53	8.81 ± 0.94	30.2 3± 5.03
50 μg mL^{-1} irr. after 24 h	37.93 ± 4.14	7.06 ±1.34	6.54 ± 0.64	48.55 ± 2.04
125 μg mL^{-1} not irr.	55.88 ± 3.88	2.41 ± 0.59	37.38 ± 2.63	4.34 ± 0.67
125 μg mL^{-1} irr. after 6 h	27.24 ± 2.24	2.01 ± 0.99	51.74 ± 1.74	19.02 ± 2.99
250 μg mL^{-1} not irr.	22.81 ± 2.81	3.50 ± 1.50	52.87 ± 2.87	16.92 ± 1.92
NGQD-BODIPY-Br				
50 μg mL^{-1} not irr.	91.85 ± 1.20	1.51 ± 0.70	3.29 ± 0.30	3.36 ± 0.20
50 μg mL^{-1} irr. after 6 h	88.38 ± 1.50	2.09 ± 0.40	3.08 ± 0.37	6.45 ± 1.47
50 μg mL^{-1} irr. after 24 h	89.57 ± 0.81	1.26 ± 0.34	4.56 ± 0.63	4.61 ± 0.16
125 μg mL^{-1} not irr.	90.91 ± 1.27	2.71 ± 0.13	2.67 ± 0.90	3.21 ± 0.21
125 μg mL^{-1} irr. after 6 h	83.73 ± 1.61	1.57 ± 0.72	6.38 ± 1.58	8.32 ± 0.69
125 μg mL^{-1} irr. after 24 h	81.00 ± 0.96	2.36 ± 0.52	6.17 ±0.24	10.47 ± 0.21
250 μg mL^{-1} not irr.	88.38 ± 0.44	4.06 ± 0.16	4.08 ± 1.05	3.48 ± 0.44
250 μg mL^{-1} irr. after 6 h	68.57± 3.22	3.755 ± 0.12	8.74 ± 1.01	18.94 ± 4.36
250 μg mL^{-1}irr. after 24 h	14.50± 2.12	8.81 ± 1.69	45.81 ± 1.68	30.89 ± 1.26

Confocal Fluorescence Cell Images

Control of the formation of ROS without irradiation was carried out. No fluorescence was detected in the ROS channel, confirming the reduced state and that irradiation is needed to form singlet oxygen, leading to apoptosis and necrosis of cancer cells.

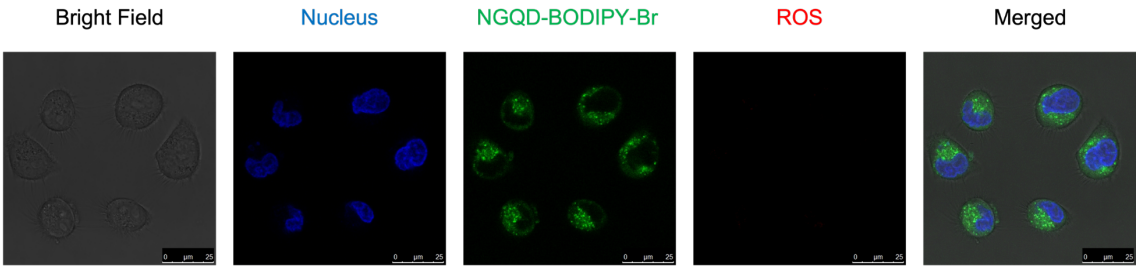

Figure S29. Confocal fluorescence cell images of HeLa cells incubated with 250 µg mL^{-1} of NGQD-BODIPY-Br not irradiated. Scale bars: 25 µm

8. References

1 P. Kaiser, E.; Colescot, R.; Bossinge, C.; Cook, Color Test for Dectection of Free Terminal Amino Groups in the Solid-Phase Synthesis of Peptides, *Anal. Biochem.*, 1970, **34**, 595–598.

2 I. J. Gómez, M. Vázquez Sulleiro, A. Dolečková, N. Pizúrová, J. Medalová, R. Roy, et al., Exploring the Emission Pathways in Nitrogen-Doped Graphene Quantum Dots for Bioimaging, *J. Phys. Chem. C*, 2021, **125**, 21044–21054.

3 E. M. Sánchez-Carnerero, M. Russo, A. Jakob, L. Muchová, L. Vítek and P. Klán, Effects of Substituents on Photophysical and CO-Photoreleasing Properties of 2,6-Substituted meso-Carboxy BODIPY Derivatives, *Chemistry*, 2021, **3**, 238–255.

4 Y. Zheng, Y. Jiao, L. Ge, M. Jaroniec and S. Z. Qiao, Two-step boron and nitrogen doping in graphene for enhanced synergistic catalysis, *Angew. Chemie - Int. Ed.*, 2013,

52, 3110–3116.

5 J. Raymakers, H. Krysova, A. Artemenko, J. Čermák, S. S. Nicley, P. Verstappen, et al., Functionalization of boron-doped diamond with a push-pull chromophore via Sonogashira and CuAAC chemistry, *RSC Adv.*, 2018, **8**, 33276–33290.

6 K. Wang, Y. Xiao, Y. Wang, Y. Feng, C. Chen, J. Zhang, et al., Self-assembled hydrophobin for producing water-soluble and membrane permeable fluorescent dye, *Sci. Rep.*, 2016, **6**, 1–11.

7 W. S. Zou, W. L. Kong, Q. C. Zhao, J. Zhang, X. Zhao, D. Zhao, et al., A composite consisting of bromine-doped carbon dots and ferric ions as a fluorescent probe for determination and intracellular imaging of phosphate, *Microchim. Acta*, , DOI:10.1007/s00604-019-3700-6.

8 D. K. Ji, G. Reina, S. Guo, M. Eredia, P. Samorì, C. Ménard-Moyon, et al., Controlled functionalization of carbon nanodots for targeted intracellular production of reactive oxygen species, *Nanoscale Horizons*, 2020, **5**, 1240–1249.